Class. Quantum Grav. **24** (2007) S381–S388 doi:10.1088/0264-9381/24/19/S01

Status of Virgo detector

F Acernese[1], P Amico[2], M Alshourbagy[3], F Antonucci[4], S Aoudia[5], P Astone[4], S Avino[1], D Babusci[6], G Ballardin[7], F Barone[1], L Barsotti[3], M Barsuglia[8], F Beauville[9], S Bigotta[3], S Birindelli[3], M A Bizouard[8], C Boccara[10], F Bondu[5], L Bosi[2], C Bradaschia[3], S Braccini[3], A Brillet[5], V Brisson[8], D Buskulic[9], E Calloni[1], E Campagna[11], F Carbognani[7], F Cavalier[8], R Cavalieri[7], G Cella[3], E Cesarini[11], E Chassande-Mottin[5], N Christensen[7], C Corda[3], A Corsi[4], F Cottone[2], A-C Clapson[8], F Cleva[5], J-P Coulon[5], E Cuoco[7], A Dari[2], V Dattilo[7], M Davier[8], M del Prete[3], R De Rosa[1], L Di Fiore[1], A Di Virgilio[3], B Dujardin[5], A Eleuteri[1], I Ferrante[3], F Fidecaro[3], I Fiori[3], R Flaminio[7,9], J-D Fournier[5], S Frasca[4], F Frasconi[3], L Gammaitoni[2], F Garufi[1], E Genin[7], A Gennai[3], A Giazotto[3], G Giordano[6], L Giordano[1], R Gouaty[9], D Grosjean[9], G Guidi[11], S Hebri[7], H Heitmann[5], P Hello[8], S Karkar[9], S Kreckelbergh[8], P La Penna[7], M Laval[5], N Leroy[8], N Letendre[9], B Lopez[7], M Lorenzini[11], V Loriette[10], G Losurdo[11], J-M Mackowski[12], E Majorana[4], C N Man[5], M Mantovani[3], F Marchesoni[2], F Marion[9], J Marque[7], F Martelli[11], A Masserot[9], M Mazzoni[11], L Milano[1], F Menzinger[7], C Moins[7], J Moreau[10], N Morgado[12], B Mours[9], F Nocera[7], C Palomba[4], F Paoletti[3,7], S Pardi[1], A Pasqualetti[7], R Passaquieti[3], D Passuello[3], F Piergiovanni[11], L Pinard[12], R Poggiani[3], M Punturo[2], P Puppo[4], K Qipiani[1], P Rapagnani[4], V Reita[10], A Remillieux[12], F Ricci[4], I Ricciardi[1], P Ruggi[7], G Russo[1], S Solimeno[1], A Spallicci[5], M Tarallo[3], M Tonelli[3], A Toncelli[3], E Tournefier[9], F Travasso[2], C Tremola[3], G Vajente[3], D Verkindt[9], F Vetrano[11], A Viceré[11], J-Y Vinet[5], H Vocca[2] and M Yvert[9]

[1] INFN, sezione di Napoli and/or Università di Napoli 'Federico II' Complesso Universitario di Monte S.Angelo, and/or Università di Salerno, Fisciano (Sa), Italy
[2] INFN, Sezione di Perugia and/or Università di Perugia, Perugia, Italy
[3] INFN, Sezione di Pisa and/or Università di Pisa, Pisa, Italy
[4] INFN, Sezione di Roma and/or Università 'La Sapienza', Roma, Italy
[5] Departement Artemis-Observatoire de la Côte d'Azur, BP 42209 06304 Nice, Cedex 4, France
[6] INFN, Laboratori Nazionali di Frascati, Frascati (Rm), Italy
[7] European Gravitational Observatory (EGO), Cascina (Pi), Italy
[8] LAL, Univ Paris-Sud, IN2P3/CNRS, Orsay, France
[9] Laboratoire d'Annecy-le-Vieux de Physique des Particules (LAPP), IN2P3/CNRS, Université de Savoie, Annecy-le-Vieux, France
[10] ESPCI, Paris, France
[11] INFN, Sezione di Firenze/Urbino, Sesto Fiorentino, and/or Università di Firenze, and/or Università di Urbino, Italy
[12] LMA, Villeurbanne, Lyon, France

E-mail: gabriele.vajente@sns.it

Received 31 March 2007, in final form 21 May 2007
Published 19 September 2007
Online at stacks.iop.org/CQG/24/S381

Abstract

The commissioning of the Virgo gravitational wave detector has restarted after several major hardware upgrades carried out during winter 2005. Now Virgo is fully operative and its sensitivity greatly improved and continually improving. A program of short scientific data taking has already started and Virgo is moving towards a period of continuous data taking, which should start at the end of May 2007. The actual status of the Virgo detector is reported, describing the actual detector sensitivity as well as the limiting noises and the mid-term plans.

PACS numbers: 04.80.Nn, 95.55.Ym

(Some figures in this article are in colour only in the electronic version)

1. Introduction

The Virgo gravitational wave detector, jointly funded by INFN (Italy) and CNRS (France) and located at the European Gravitational Observatory (EGO) near Pisa, is a power recycled Michelson interferometer with arms composed of 3 km long Fabry–Perot resonant cavities [1]. A schematic optical layout is shown in figure 1. The input beam is generated by a 20 W high-power Nd:YVO_4 laser locked to a 1 W solid state Nd:YAG master laser. The beam enters the vacuum system and passes through a 144 m long input mode cleaner (IMC) which is used both for spatial filtering of the beam and for pre-stabilization of the laser frequency. A small fraction of the beam is sent to the rigid reference cavity (RFC), used as a frequency reference. The beam then enters the main interferometer, consisting of a power recycling mirror (PR), a beam splitter (BS) and two resonant cavities with flat input mirrors (NI and WI) and curved terminal mirrors (NE and WE). The beams transmitted by the cavity end mirrors are sensed by both photodiodes and quadrant split photodiodes: the signals obtained from the former are used in the earlier stages of lock acquisition [2], while those from the latter are used for automatic alignment purposes, since in Virgo the main modulation frequency is chosen in order to be resonant in the recycling cavity and to make the upper sideband first transverse mode resonant in the arm cavities [3]. The beams reflected by the secondary anti-reflection-coated surface of the beam splitter and by the power recycling mirror are also sent outside the vacuum and sensed by photodiodes and quadrant split photodiodes.

The main output beam coming from the recombination at the beam splitter passes through an output mode cleaner (OMC) which is suspended in a vacuum, in order to improve the interferometer contrast by filtering out high order modes. The demodulation of this beam gives the gravitational wave output signal.

All the mirrors are suspended by multi-stage passive seismic isolation systems (*superattenuators* [4]) which can be controlled by both local and global signals depending on the interferometer control condition.

2. Hardware modification during winter 2005 shutdown

A three-month shutdown took place just after the C7 commissioning run, starting from mid September 2005 and ending in December of the same year. During this period two main hardware changes were carried out: the power recycling mirror and the whole suspended injection bench have been replaced.

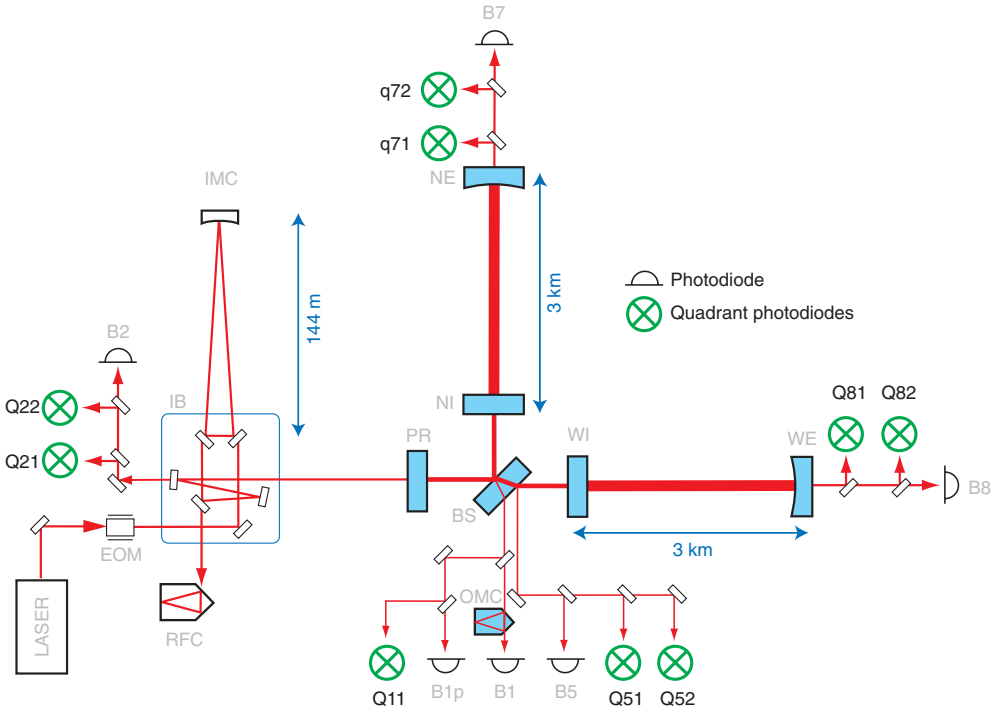

Figure 1. A simplified scheme of the Virgo optical layout. See the text for details.

2.1. Power recycling mirror

The initial power recycling suspended mirror was a compound one, with a curved secondary surface to form the last part of the input beam mode-matching telescope. The main drawback of this compound mirror was that it showed internal resonances between 100 Hz and 500 Hz that made the design of the ITF control system more difficult.

The new mirror, instead, is monolithic, flat and has a higher reflectivity (95% instead of 92%). Apart from the expected increase of recycling gain due to the increased reflectivity, the new mirror allowed a strong improvement in the performances of the longitudinal control system, due to the absence of internal resonances (see figure 2).

2.2. New suspended injection bench

Before the shutdown, the suspended injection bench included a partially reflecting mirror which was used to attenuate the power entering the interferometer by a factor of 10. This was necessary to avoid back-reflected light interfering inside the IMC, spoiling the control of this cavity and the level of laser frequency noise. The new injection bench (see figure 3) has been designed including a Faraday isolator placed in transmission of the IMC, in order to inject the full power inside the ITF and avoid the aforementioned problem. This isolator gives an attenuation of the beam coming back by a factor of roughly 1000, which has been proved to be sufficient. Another feature of the new injection bench is the telescope used for matching the beam with the resonant mode of the interferometer: this telescope is composed of two parabolic mirrors and has been designed in order to reduce the astigmatism of the beam as

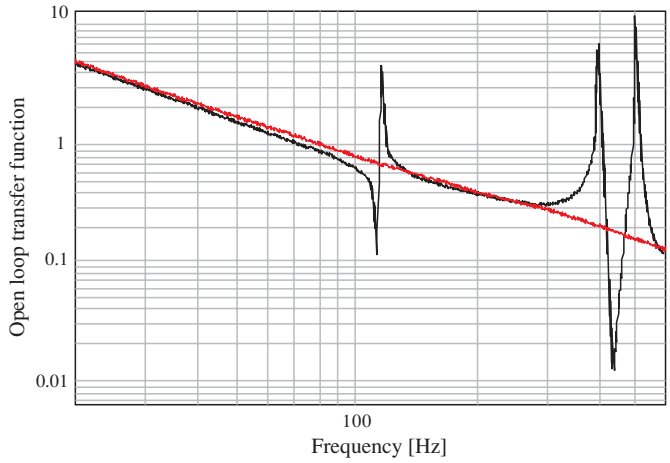

Figure 2. Comparison of the open loop transfer function for the longitudinal control of a cavity composed by the PR mirror and the NI mirror. The black curve shows a measurement performed with the old power recycling mirror, while the red curve is a measurement with the new mirror. Internal resonances of the compound PR mirror are well visible in the former measurement.

much as possible. The last important point to note is the photodiode used for stabilizing the laser power, which is now placed on this suspended bench, in a vacuum, in transmission of the IMC.

2.3. Acoustic isolation

During another shorter shutdown, in September 2006, an acoustic isolation shielding was installed around the laser bench and the external injection bench. Several tests performed after this operation show a relevant reduction of acoustic noise contamination of the dark fringe signal.

3. Commissioning restart

The main challenge in recovering a stable lock of the interferometer after these major changes was the appearance of thermal effects in the final steps of the lock acquisition sequence. When the interferometer is finally brought to dark fringe, meaning that the full power build-up takes place in the arm cavities, the two input mirrors start to heat up, changing the interferometer state and response. This effect made the development of a working lock acquisition strategy more difficult and the interferometer strongly sensitive to the amount of input power. We were forced to decrease the power injected inside the interferometer, which is now about 7.9 W. In this condition it is possible to acquire the lock, but the full sequence takes about 20 minutes, due to the need to wait for the mirrors to thermalize.

4. Weekend science runs

In September 2006, a program of short science data taking (weekend science run, WSR) started. On average twice per month a full weekend, starting on Friday night until Monday morning, is dedicated to continuous data taking, with the interferometer locked in the best possible configuration. The main goals of this WSR program are to take periodic pictures

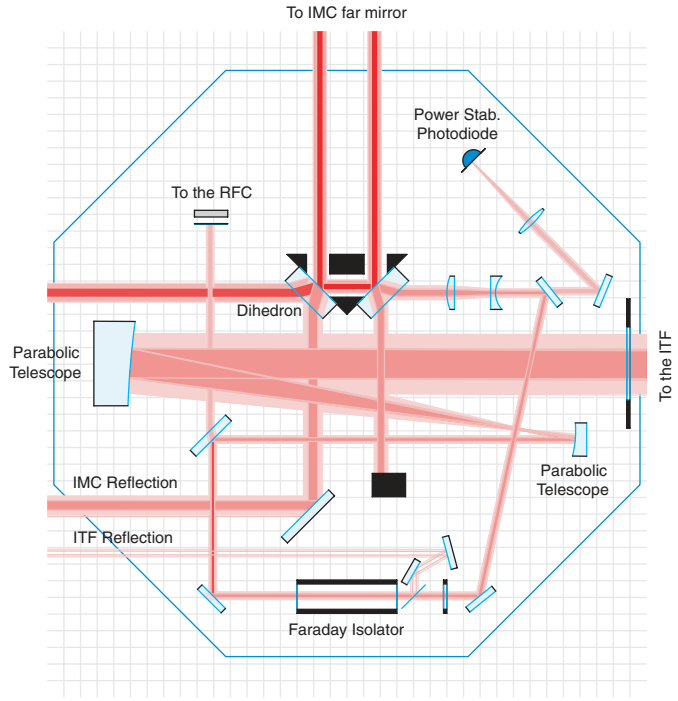

Figure 3. Simplified scheme of the new suspended injection bench. Note the mode-matching parabolic telescope, the suspended photodiode for laser power stabilization placed in transmission of the IMC and the Faraday isolator.

Table 1. The dates and duty cycles of past WSR runs.

Run	Date	Duty cycle
WSR1	8–11 September 2006	88%
WSR2	22–25 September 2006	69%
WSR3	6–9 October 2006	Cancelled
WSR4	13–16 October 2006	Cancelled
WSR5	10–13 November 2006	62%
WSR6	1–4 December 2006	81%
WSR7	12–17 January 2007	76%
WSR8	9–12 February 2007	92%
WSR9	17–19 February 2007	100%
WSR10	9–12 March 2007	60%

of the state and sensitivity of the detector, to track the improvement in sensitivity, robustness and duty cycle, to collect some data in clean and controlled conditions (to be used for both commissioning and data analysis purposes) and to start moving towards the organization needed for a longer science run. It must be noted that the priority always remains on the commissioning activities, and therefore a WSR run can be cancelled or postponed if the detector is not in good working condition or if there are other needs.

So far, ten weekend science runs have been performed (refer to table 1 for their dates). Two of these have been cancelled due to bad working conditions of the interferometer. All the others had quite a good duty cycle and the longest lock obtained so far was that of WSR9, when

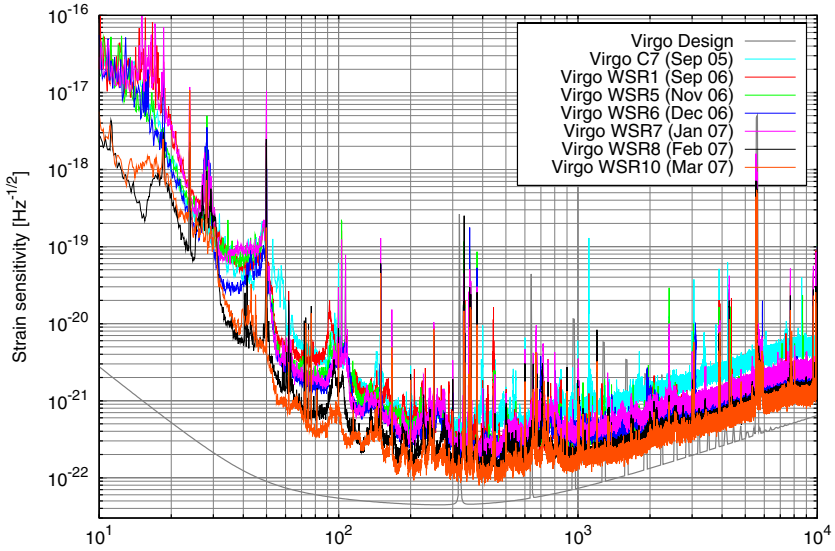

Figure 4. Strain sensitivity of the Virgo detector during some of the WSR runs, compared to that of the C7 commissioning run. The light grey curve is the Virgo design sensitivity.

the detector was stably locked for more than 55 hours. The main factor limiting the stability of the interferometer is linked to environmental conditions, mainly micro-seismic activity due to the sea and wind. A lot of effort has been devoted to improving this situation: during the first runs it was difficult to acquire the lock with strong wind and sea activity, while now the situation is much improved: the sensitivity, however, is still slightly varying in dependence of the micro-seismic conditions.

In figure 4, it is possible to see the improvements in sensitivity obtained during the last months, compared to that of the last Virgo commissioning run C7 which took place in September 2005. The improvements in the high frequency region (above 1 kHz) are due to the increases of laser power between C7 and WSR1 and to the better matching of the beam and a reduced frequency noise coupling for the other WSR runs. The improvements in the intermediate frequency region (between 200 Hz and 1 kHz) are due to the large efforts carried out to reduce contamination by diffused and back-scattered light that can couple with acoustic noise and seismic vibrations of the external benches. The improvement between 50 Hz and 200 Hz between the first WSR runs and WSR7 is due to the use of a different and less noisy error signal for the control of one of the longitudinal degrees of freedom, namely the length of the power recycling cavity. Great improvements in the stability and accuracy of the angular control servos helped to reduce the low frequency RMS motion of the interferometer, allowing a better tuning of the longitudinal control systems. This resulted in the improvements visible between WSR7 and WSR8, when a frequency-dependent noise subtraction technique was used. Finally, before the start of WSR10 run a source of electromagnetic noise has been found and reduced, resulting in the strong suppression of noise in the region around 100 Hz.

5. Noise performances

There are several sources of noise that limit the sensitivity (see figure 5). At low frequency (between 10 and 50 Hz), the dominating source of noise comes from the longitudinal control

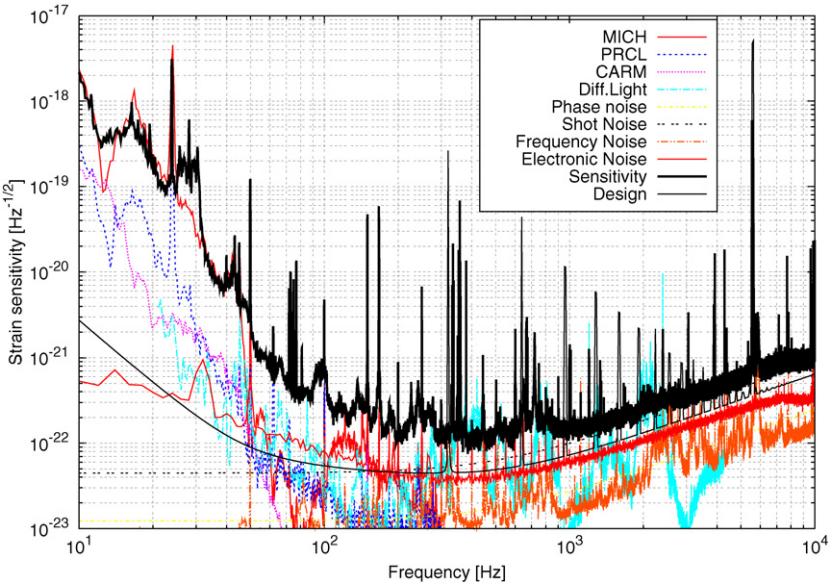

Figure 5. Noise budget for the WSR10 run. MICH, PRCL and CARM curves refer to longitudinal control noise, respectively, for the short Michelson, power recycling cavity length and long cavities common mode degrees of freedom. The shot noise is computed taking into account the actual power circulating in the interferometer. Electronic and phase noises are estimated using analytical models (so far no measurement has been performed). The diffused light curve shows an example of projections of acoustic and seismic excitation of external benches, estimated using noise injection.

servos, mainly the one controlling the short Michelson degree of freedom. Angular control noise is for the moment below the actual sensitivity, and for most of the angular degrees of freedom the contribution to dark fringe noise is even below the design sensitivity above 30–40 Hz. The noise at high frequency (above 1 kHz) is also quite well understood, and it comes mainly from shot noise at dark fringe and frequency noise in a small region around 6 kHz. The noise in the intermediate region, between 50 Hz and up to 1 kHz, is likely to be due to acoustic noise and seismic noise at the level of the external benches, reintroduced due to diffused and scattered light.

The stability and stationarity of the detector noise has also greatly improved during recent months, allowing stable and repeatable operation of the detector.

6. Conclusions

The Virgo detector sensitivity has reached a level comparable to that of the LSC detectors above 500 Hz (see figure 6), and very close in the remaining part of the observational bandwidth. Therefore, the main goal of the Virgo collaboration is to join the LSC detectors for a coincident data taking period. This first long Virgo science run started on 18th May and is planned to continue for several months, at least until the end of the LIGO S5 run.

Before the beginning of the science run, the main task for the commissioning remains to improve the detector sensitivity and duty cycle as much as possible. Main activities concern control noise characterization and possible reduction for the low frequency region, acoustic shielding installation in the detection laboratory and substitution of critical optical elements

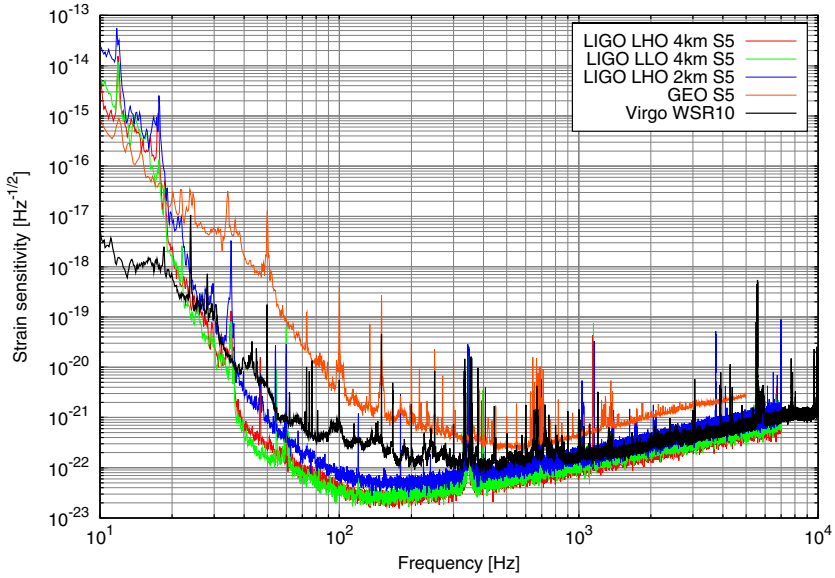

Figure 6. Comparison of the Virgo sensitivity during WSR10 with that of the LSC detectors during S5 run.

to reduce acoustic and seismic noise contamination due to diffused and scattered light, and implementation of new electronics for the laser frequency stabilization servo.

These modifications should allow for further improvement of the sensitivity, reaching the level of the other detectors even in the frequency region between 50 Hz and 500 Hz.

References

[1] http://www.virgo.infn.it
[2] Acernese F *et al* (Virgo Collaboration) 2006 The variable finesse locking technique *Class. Quantum Grav.* **23** S85
[3] Acernese F *et al* (Virgo Collaboration) 2006 The Virgo automatic alignment system *Class. Quantum Grav.* **23** S91
[4] Acernese F *et al* (Virgo Collaboration) 2005 Measurement of the seismic attenuation performance of the Virgo superattenuator *Astropart. Phys.* **23** 557–65